Decision Feedback Differential Phase Detection of M-ary DPSK Signals

Fumiyuki Adachi, *Senior Member, IEEE*, and Mamoru Sawahashi, *Member, IEEE*

Abstract— **Multiple-symbol differential phase detection (DF-DPD) based on decision feedback of past detected symbols is presented for M-ary DPSK modulation. Adopting a Gaussian phase noise assumption, we obtain the *a posteriori* joint probability density function (pdf) of the outputs of L DPD detectors of orders of 1 to L symbols and derive a DF-DPD algorithm which is based on feeding back the $L-1$ past detected symbols and minimizing the sum of phase errors of L DPD detectors. A practical implementation of the DF-DPD receiver is presented that uses a single conventional (one-symbol) DPD detector. The bit error rate (BER) performance in an additive white Gaussian noise (AWGN) channel is analyzed taking into account decision error propagation. Performance improvements are evaluated by computer simulations in AWGN and Rayleigh fading channels.**

I. Introduction

M-ARY differential phase shift keying (DPSK) is a bandwidth efficient digital modulation technique, and recently has attracted increased attention in mobile radio where the available radio bandwidth is limited. Coherent detection offers good bit error rate (BER) performance in additive white Gaussian noise (AWGN) channels. However, it requires long acquisition times and, in fading environments, exhibits poor BER performance due to fast variations in the received signal phase; thus, differential detection is preferred. In AWGN channels, however, the BER performance of differentially detected M-ary DPSK is inferior to that of coherent detection. This is because a delayed version of the received noisy signal is used as the phase reference. To narrow the performance gap between differential and coherent detection, several multiple-symbol differential detection schemes have been proposed: maximum likelihood differential detection (ML-DD) [1], ML-DD using Viterbi algorithm (Viterbi-DD) [2]–[4], and decision feedback differential detection (DF-DD) [5], [6]. ML-DD makes a decision about a block of L consecutive symbols from $L+1$ received signal samples, based on maximum likelihood sequence estimation. Viterbi-DD is a simplification of the original ML-DD and uses L differential detectors of orders of 1 to L symbols. DF-DD is a symbol-by-symbol detection scheme based on feeding back the $L-1$ past detected symbols. The larger the value of L, the better the BER performance. At the limit of $L \to \infty$, its performance approaches that of coherent detection with differential decoding (in this paper, referred to as CD) to resolve phase ambiguity. When $L = 1$, all ML-, Viterbi-, and DF-DD schemes reduce to conventional (one-symbol) DD. However, the above mentioned schemes need to preserve the amplitude variation of the AWGN-perturbed received signal; thus limiter amplifiers, in the practical receivers placed between IF bandpass filtering and differential detection, cannot be applied. Furthermore, a number of two-dimensional (complex-valued) multiply-and-add operations is necessary. Therefore, implementation of these multiple-symbol DD schemes is not simple.

It is well known that the differential detector can also be implemented using a phase detector. The phase of the received signal plus noise is detected and the phase difference is used for decision. This is called differential phase detection (DPD). Conventional DPD uses the phase difference over one symbol duration. We note [7] that although DF-DD is much simpler than ML- and Viterbi-DD, its BER performance is close to that of ML-DD using the same L. Because of the rather encouraging performance of DF-DD, we apply the idea of decision feedback to the DPD scheme. This scheme is called DF-DPD in this paper. This paper is organized as follows. In Section II, we adopt a Gaussian phase noise assumption, and derive a DF-DPD algorithm which is based on feeding back the $L-1$ past detected symbols and minimizing the sum of phase errors of L DPD detectors. Also shown is a practical implementation of the algorithm that uses conventional DPD detector output only. Section III gives an approximate analysis of its BER performance in AWGN channels taking into account the decision error propagation effect. Performance improvements are evaluated by computer simulations for 2DPSK and 4DPSK transmission in AWGN and Rayleigh fading channels and the results are presented in Section IV.

II. DF-DPD Algorithm

A. Received Signal and Conventional DPD

The M-ary DPSK signal to be transmitted can be represented in the complex form as

$$s(t) = \sqrt{\frac{2E_s}{T}} \sum_{n=-\infty}^{\infty} p(t-nT)e^{j\phi_n} \tag{1}$$

where $\phi_n = \{2m\pi/M;\ m = 0, 1, \cdots, M-1\}$ is the modulation phase, E_s is the signal energy per symbol, T is the symbol duration, and $p(t)$ is the lowpass equivalent impulse response of the transmit filter (we assume a square

Manuscript received July 21, 1993; revised April 7, 1994.

The authors are with the Department of Research and Development, NTT Mobile Communications Network, Inc., Yokosuka-shi, Kanagawa-ken, 238 Japan.

IEEE Log Number 9407331.

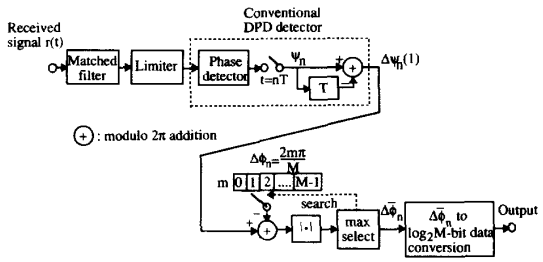

Fig. 1. Conventional DPD receiver.

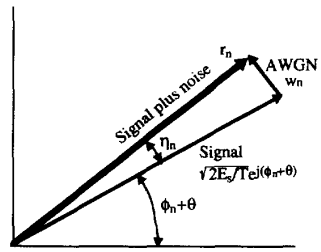

Fig. 2. Phasor diagram of the received signal.

root Nyquist filter). The phase difference $\Delta\phi_n = \phi_n - \phi_{n-1}$ represents the transmitted $\log_2 M$-bit symbol. The M-ary DPSK signal is assumed to be transmitted and received over an AWGN channel. The receiver structure employing conventional DPD is shown in Fig. 1. We assume, as in [5], perfect automatic frequency control (AFC) such that there is no frequency offset between the transmitter and receiver and perfect sampling timing. The received signal is perturbed by the AWGN with single-sided power spectrum density N_0 and is bandlimited by the receive matched filter with lowpass equivalent impulse response $h(t) = (1/T)p(-t)$. The receive filter output can be expressed as

$$r(t) = \tilde{s}(t) \exp j\theta + w(t) \tag{2}$$

where $\tilde{s}(t) = s(t) \otimes h(t)$ is the receive filter response to $s(t)$ (here, $\otimes$ is the convolution operation), θ is the unknown phase offset, and $w(t)$ is the filtered AWGN component. We assume that θ is constant over the time interval $(n-L-1)T < t \leq nT$ with L being an integer, where the time interval $(L+1)T$ represents the observation length for making a decision. After amplitude limiting, the phase of the filtered signal plus noise $r(t)$ is detected by the phase detector and sampled at $t = nT$; the sampled phase is denoted by ψ_n. Since overall (transmit plus receive) filter response forms an intersymbol interference (ISI)-free Nyquist filter response at the sampling instant (i.e., $\tilde{s}(nT) = \sqrt{2E_s/T} \exp j\phi_n$), $\psi_n = \arg(r_n)$, where

$$r_n = r(nT) = \sqrt{\frac{2E_s}{T}} e^{j(\phi_n + \theta)} + w_n \tag{3}$$

with $w_n = w(nT)$ being the zero-mean complex Gaussian noise sample with variance $E(|w_n|^2) = 2N_0/T$. The phasor diagram of the received signal is shown in Fig. 2. Denoting the AWGN-induced phase noise by η_n, ψ_n can be expressed as

$$\psi_n = (\phi_n + \eta_n + \theta) \bmod 2\pi. \tag{4}$$

The conventional DPD detector produces the phase difference of successive two phases:

$$\Delta\psi_n(1) = (\psi_n - \psi_{n-1}) \bmod 2\pi. \tag{5}$$

At this stage, the unknown phase θ is removed. The conventional DPD decision is to find the phase difference $\Delta\bar{\phi}_n$ from $\{2m\pi/M;\ m = 0, 1, \cdots, M-1\}$ that is closest to $\Delta\psi_n(1)$. The transmitted $\log_2 M$-bit symbol is then recovered from $\Delta\bar{\phi}_n$. Since the reference phase of conventional DPD, as shown in (5), is ψ_{n-1} which is perturbed by AWGN, its BER performance is inferior to that of CD.

B. DF-DPD Algorithm

A total of L DPD detectors of orders of 1 to L symbols is used to make a decision on the transmitted symbol $\Delta\phi_n$. Using (4) and the relation

$$\phi_n = \left(\phi_{n-l} + \sum_{i=0}^{l-1} \Delta\phi_{n-i}\right) \bmod 2\pi \tag{6}$$

the output of an l-symbol DPD detector can be expressed as

$$\begin{aligned}\Delta\psi_n(l) &= (\psi_n - \psi_{n-l}) \bmod 2\pi \\ &= \left(\sum_{i=0}^{l-1} \Delta\phi_{n-i} + \Delta\eta_n(l)\right) \bmod 2\pi\end{aligned} \tag{7}$$

where $\Delta\eta_n(l) = \eta_n - \eta_{n-l}$ is the differential phase noise. It is shown in the Appendix that for large values of E_s/N_0, η_{n-l}'s can be approximated as uncorrelated, zero-mean Gaussian variables with the same variance $0.5(E_s/N_0)^{-1}$. From this and noting that all $\Delta\eta_n(l)$'s contain the phase noise η_n in common, $\Delta\eta_n(l)$ are found to be approximately, jointly Gaussian distributed. The covariance matrix $\boldsymbol{R} = \langle \boldsymbol{\Delta\eta}^T \boldsymbol{\Delta\eta} \rangle$ of $\boldsymbol{\Delta\eta} = (\Delta\eta_n(1), \Delta\eta_n(2), \cdots, \Delta\eta_n(L))$, where $(\cdot)^T$ is the transpose, has the elements

$$R_{ij} = \langle \Delta\eta_n(i) \Delta\eta_n(j) \rangle = \begin{cases} \left(\frac{E_s}{N_0}\right)^{-1} & \text{if } i = j \\ 0.5\left(\frac{E_s}{N_0}\right)^{-1} & \text{otherwise} \end{cases} \tag{8}$$

where $i, j = 1, 2, \cdots, L$. Therefore, it can be shown from (7) that for large E_s/N_0, the *a posteriori* joint pdf $p(\boldsymbol{\Delta\psi} \mid \boldsymbol{\Delta\phi})$ of $\boldsymbol{\Delta\psi} = (\Delta\psi_n(1), \Delta\psi_n(2), \cdots, \Delta\psi_n(L))$ given that $\boldsymbol{\Delta\phi} = (\Delta\phi_n, \Delta\phi_{n-1}, \cdots, \Delta\phi_{n-L+1})$ has been sent can be approximated as

$$p(\boldsymbol{\Delta\psi} \mid \boldsymbol{\Delta\phi}) = \frac{1}{(2\pi)^{L/2} (\det \boldsymbol{R})^{1/2}} \exp\left[-\frac{\boldsymbol{\mu}^T \boldsymbol{R}^{-1} \boldsymbol{\mu}}{2}\right] \tag{9}$$

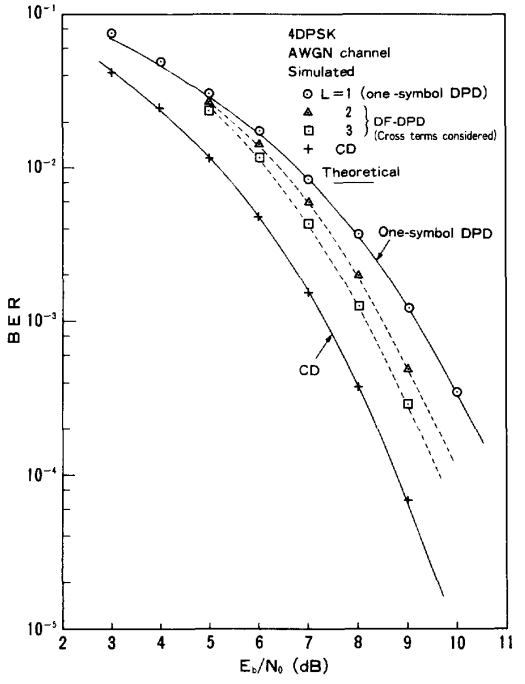

Fig. 3. BER performance of DF-DPD using $L = 2$ and 3. Cross terms are considered.

where $\det \boldsymbol{R}$ and $\boldsymbol{R}^{-1}$ are the determinant and the inverse of $\boldsymbol{R}$, respectively, and $\boldsymbol{\mu} = (\mu_1, \mu_2, \cdots, \mu_L)$ with $\mu_l = \left(\Delta\psi_n(l) - \sum_{i=0}^{l-1}\Delta\phi_{n-i}\right) \bmod 2\pi$ is the phase error vector of L DPD detectors. The optimal decision is to find the sequence $\boldsymbol{\Delta\phi}$ that maximizes (9). However, we want to derive a symbol-by-symbol decision algorithm for $\Delta\phi_n$. Here, we feedback the $L-1$ past detected symbols $\Delta\bar{\phi}_{n-l}$, $l = 1, 2, \cdots, L-1$, and use them instead of $\Delta\phi_{n-l}$. We substitute

$$\mu_l = \left(\Delta\psi_n(l) - \Delta\phi_n - \sum_{i=1}^{l-1}\Delta\bar{\phi}_{n-i}\right) \bmod 2\pi \tag{10}$$

in (9) and obtain a DF-DPD algorithm based on maximizing $p(\boldsymbol{\Delta\psi} \mid \Delta\phi_n, \Delta\bar{\phi}_{n-1}, \cdots, \Delta\bar{\phi}_{n-L+1})$. Taking the logarithm of $p(\boldsymbol{\Delta\psi} \mid \Delta\phi_n, \Delta\bar{\phi}_{n-1}, \cdots, \Delta\bar{\phi}_{n-L+1})$ and neglecting the constants which do not affect the maximization, we arrive at the following decision rule:

$$\Delta\bar{\phi}_n = \min_{\text{over } \Delta\phi_n} \boldsymbol{\mu}^T \boldsymbol{R}^{-1} \boldsymbol{\mu}. \tag{11}$$

In particular, for $L = 2$ and 3, (11) simplifies to (12), as shown at the bottom of the page. We computer-simulated DF-DPD using $L = 2$ and 3 to determine the performance improvements for 4DPSK ($M = 4$) in AWGN channels. The results are plotted in Fig. 3 as a function of the signal energy per bit-to-noise power spectrum density ratio E_b/N_0 ($= (E_s/N_0)/\log_2 M$). For comparison, we plotted the theoretical performance of conventional DPD ($L = 1$) and that of CD [the BER's are given by (24)]. It can be seen that DF-DPD using $L = 2$ (3) can achieve a 0.64 (1.0) dB improvement over conventional DPD at BER $= 10^{-3}$.

As seen in (12), the decision feedback algorithm involves computation of the cross terms of the phase errors. Since the cross terms can take positive and negative values, their effect on decision may be negligible on average. Computer simulation confirmed this (no performance difference was observed below $E_b/N_0 = 9$ dB). This greatly simplifies the algorithm. The simplified algorithm is based on minimizing the sum of the squared phase errors of multiple l-symbol DPD detectors. This corresponds to approximating the correlation matrix $\boldsymbol{R}$ as a diagonal matrix with elements of $R_{ij} = (E_s/N_0)^{-1}$ if $i = j$ and $= 0$ otherwise. Thus, the decision rule for $\Delta\phi_n$ simplifies to

$$\Delta\bar{\phi}_n = \min_{\text{over } \Delta\phi_n} \sum_{l=1}^{L} \mu_l^2. \tag{13}$$

Hereafter, we refer to this algorithm simply as DF-DPD.

C. Implementation of DF-DPD Receiver

The direct implementation of the DF-DPD receiver requires L multiple-symbol DPD detectors of orders of 1 to L symbols. However, we can show that all μ_l's are generated from the single conventional DPD detector. Using the relation

$$\Delta\psi_n(l) = \left(\sum_{i=1}^{l-1}\Delta\psi_{n-i}(1)\right) \bmod 2\pi \tag{14}$$

μ_l can be generated in the recursive form as

$$\mu_l = (\mu_{l-1} + [\Delta\psi_{n-l+1}(1) - \Delta\bar{\phi}_{n-l+1}]) \bmod 2\pi \tag{15}$$

where $\mu_1 = (\Delta\psi_n(1) - \Delta\phi_n) \bmod 2\pi$ and $\Delta\psi_n(1)$ is the conventional DPD detector output. Noting that $[\Delta\bar{\psi}_{n-l+1}(1) - \Delta\phi_{n-l+1}]$ is the phase error associated with the past decision at $t = (n-l+1)T$, a simplified DF-DPD algorithm can be derived and is shown in Fig. 4. It should be pointed out that the DF-DPD algorithm can be added to the conventional DPD receiver, and therefore, it is considered very practical.

$$\Delta\bar{\phi}_n = \begin{cases} \min\limits_{\text{over } \Delta\phi_n} \mu_1^2 + \mu_2^2 - \mu_1\mu_2 & \text{for } L = 2 \\ \min\limits_{\text{over } \Delta\phi_n} \mu_1^2 + \mu_2^2 + \mu_3^2 - \frac{2}{3}(\mu_1\mu_2 + \mu_1\mu_3 + \mu_2\mu_3) & \text{for } L = 3 \end{cases} \tag{12}$$

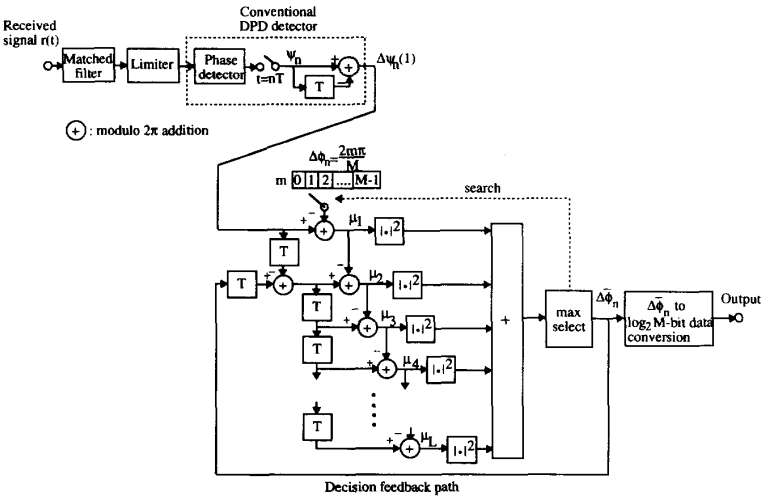

Fig. 4. Implementation of DF-DPD receiver.

III. BER Analysis

The decision feedback algorithm utilizing detected symbols to provide a reference introduces problems of error propagation; previous decision error directs the reference phase towards the wrong value. We first analyze the effect of decision error propagation and then, derive an approximate BER expression for DF-DPD.

A. Error Propagation

Let $\Delta\bar{\phi}_n = \Delta\bar{\phi}_n + \delta\phi_n$, where $\delta\bar{\phi}_n = \{2m\pi/M;\ m = 0, \pm1, \pm2, \cdots, \pm(M/2-1), -M/2\}$ is the decision phase error (note that $m = 0$ corresponds to no decision error). We assume that an error has been just caused by AWGN on the nth decision, i.e., $\delta\bar{\phi}_n = 2m\pi/M$ with $m \neq 0$ and $\delta\bar{\phi}_{n-l} = 0$, $l = 1, 2, \cdots, L-1$. It can be shown from (7), (10), and (13) that the $n+1$th decision becomes

$$\delta\bar{\phi}_{n+1} = \min_{\text{over}\delta\phi_{n+1}} \sum_{l=1}^{L} |(\Delta\eta_{n+1}(l) - \delta\phi_{n+1} - \delta\bar{\phi}_n) \bmod 2\pi|^2. \quad (16)$$

Apparently, $\delta\bar{\phi}_{n+1} = -\delta\bar{\phi}_n$ with high probability, and a symbol error with the same number of bit errors as in the previous incorrect decision is produced (we assume Gray code bit mapping). Since $\delta\bar{\phi}_{n+1} + \delta\bar{\phi}_n = 0$, the $n+2$th decision will be

$$\delta\bar{\phi}_{n+2} = \min_{\text{over}\delta\phi_{n+2}} \sum_{l=1}^{L} |(\Delta\eta_{n+2}(l) - \delta\phi_{n+2}) \bmod 2\pi|^2 \quad (17)$$

which implies that the $n+2$th decision is not affected by the decision error made on the nth decision. As a consequence, once a single decision error is caused by AWGN, a double-symbol error is likely produced by error propagation (this will be confirmed by computer simulation in Section IV-A). Thus, the BER of DF-DPD, taking account of the decision error propagation effect, can be approximately given as twice that with correct symbol feedback. Note that when $L = 1$, no decision error propagation occurs.

B. BER Derivation

An approximate expression for the BER of DF-DPD with correct symbol feedback, i.e., $\delta\bar{\phi}_{n-l} = 0$, $l = 1, 2, \cdots, L-1$, is derived. From (7), (10), and (13), we define

$$\lambda(m, k) = \sum_{l=1}^{L} \left| \left(\Delta\eta_n(l) - \frac{2m\pi}{M} \right) \bmod 2\pi \right|^2 - \sum_{l=1}^{L} \left| \left(\Delta\eta_n(l) - \frac{2k\pi}{M} \right) \bmod 2\pi \right|^2 \quad (18)$$

for the nth decision, where $m, k = 0, \pm1, \pm2, \cdots, \pm(M/2-1), -M/2$. If $\lambda(m, k) < 0$ for all k but $k \neq m$, $\delta\bar{\phi}_n = 2m\pi/M$. Since, for large E_s/N_0, the phase noises $\Delta\eta_n(l)$'s are distributed within the vicinity of zero radians, the mod 2π operation in (18) can be omitted. Remembering that $\Delta\eta_n(l) = \eta_n - \eta_{n-l}$, (18) can be simplified to

$$\lambda(m, k) = -(m-k)\frac{4\pi L}{M}\left(\Delta\eta_{n,\,\text{DF}} - (m+k)\frac{\pi}{M}\right) \quad (19)$$

where

$$\Delta\eta_{n,\,\text{DF}} = \eta_n - \frac{1}{L}\sum_{l=1}^{L}\eta_{n-l}. \quad (20)$$

We can show from (19) that the decision will be $\delta\bar{\phi}_n = 2m\pi/M$ when $(2m-1)\pi/M < \Delta\eta_{n,\,\text{DF}} < (2m+1)\pi/M$. When $L = 1$, $\Delta\eta_{n,\,\text{DF}} (= \Delta\eta_n(1))$ represents the differential phase noise of the conventional DPD detector. This implies that the second term of RHS of (20) can be considered as the noise in the phase reference of the DF-DPD scheme. We define the phase reference noise as

$$\eta_{n-1,\,\text{DF}} = \frac{1}{L}\sum_{l=1}^{L}\eta_{n-l}. \quad (21)$$

As L increases, the phase reference noise is smoothed. At the limit of $L \to \infty$, it becomes zero and the BER of DF-DPD approaches that of CD.

For deriving the BER, we need to know the statistics of $\eta_{n-1,\,\mathrm{DF}}$. Since exact statistics are not available, we present here an approximate analysis. η_{n-l} is the phase noise of the received signal r_{n-l} having SNR $= E_s/N_0$. In the Appendix, it is shown that η_{n-l}'s can be approximated as uncorrelated zero-mean Gaussian variables with the same variance $0.5(E_s/N_0)^{-1}$. Since $\eta_{n-1,\,\mathrm{DF}}$ is the average of L uncorrelated zero-mean Gaussian variables, it also becomes a zero-mean Gaussian, but with a reduced variance of $0.5(L \times E_s/N_0)^{-1}$. This discussion suggests that the distribution of $\eta_{n-1,\,\mathrm{DF}}$ is close to that of the phase noise of the received signal having an improved SNR of $L \times E_s/N_0$. This approximation allows the BER to be analyzed based on Pawula *et al.*'s case 2 [8]. Since $\Delta\eta_{n-1,\,\mathrm{DF}}$ $(= \eta_n - \eta_{n-1,\,\mathrm{DF}})$ is symmetrically distributed with respect to zero, it is sufficient to consider the negative range only. Substituting $\rho_2 = E_s/N_0$ and $\rho_1 = L \times E_s/N_0$ into U, V, W of [8, (11)], the distribution of $\Delta\eta_{n,\,\mathrm{DF}}$ can be expressed as $\mathrm{Prob}[-\pi \le \Delta\eta_{n,\,\mathrm{DF}} \le \eta] = F(\eta) - F(-\pi)$ for $\eta < 0$, where

$$F(\eta) = \frac{-W\sin\eta}{4\pi} \cdot \int_{-\frac{\pi}{2}}^{\frac{\pi}{2}} \frac{\exp - [U - V\sin t - W\cos\eta\cos t]}{U - V\sin t - W\cos\eta\cos t}\,dt \quad (22)$$

with $U = (L+1)E_s/N_0$, $V = (L-1)E_s/N_0$, and $W = \sqrt{L}E_s/N_0$. For 2 DPSK, a bit error is produced when $\Delta\eta_{n,\,\mathrm{DF}} < -\pi/2$ and the BER with correct symbol feedback is given by $P_{b,\,2\mathrm{DPSK}} = 2F(-\pi/2)$. For 4DPSK, a single bit error is produced when $-3\pi/4 \le \Delta\eta_{n,\,\mathrm{DF}} < -\pi/4$ and two-bit error when $\Delta\eta_{n,\,\mathrm{DF}} < -3\pi/4$, and thus we have $P_{b,\,4\mathrm{DPSK}} = F(-\pi/4) + F(-3\pi/4)$. For $M > 4$, the probability of $\Delta\eta_{n,\,\mathrm{DF}}$ falling in error regions other than the nearest region $(-3\pi/M \le \Delta\eta_{n,\,\mathrm{DF}} < -\pi/M)$ is negligible and thus, the BER can be well approximated as $P_{b,\,\mathrm{MDPSK}} = (2/\log_2 M)F(-\pi/M)$. For large values of E_s/N_0, the limits of integration in (22) can be extended to $\pm\pi$ with negligibly small error. We should remember that in the case of $M = 2$, this extension leads to 2 times $F(-\pi/2)$ since the value of $W\cos(-\pi/2)\cos t$ always is zero. For $M = 4$, this extension gives the exact result for $F(-\pi/4)+F(-3\pi/4)$. As a consequence, taking into account decision error propagation, the BER of DF-DPD for $L \ge 2$ can be approximated as

$$P_{b,\,\mathrm{DF\text{-}DPD}} = \frac{2a(M)}{\log_2 M}\frac{\sqrt{L}\sin\frac{\pi}{M}}{L+1}\frac{1}{\pi} \cdot \int_0^{\pi} \frac{\exp\left[-\frac{E_s}{N_0}\frac{L+1}{2}\left(1 - \frac{\sqrt{L^2+2L\cos\frac{2\pi}{M}+1}}{L+1}\cos t\right)\right]}{1 - \frac{\sqrt{L^2+2L\cos\frac{2\pi}{M}+1}}{L+1}\cos t}\,dt \quad (23)$$

where $a(M) = 1$ (2) for $M = 2(\ge 4)$. Equation (23) is an approximation for $M \ge 8$.

DF-DPD reduces to conventional DPD when $L = 1$ and approaches CD as $L \to \infty$. When $L = 1$, a factor of 2 increase in the BER is not necessary because decision error propagation does not exist. For deriving the BER of CD, we can refer to [9]. The BER expressions for the two limiting cases can be given by

$$\begin{cases} P_{b,\,\text{conventional DPD}} = \frac{a(M)}{\log_2 M}\frac{\sin\frac{\pi}{M}}{2\pi} \cdot \int_0^{\pi} \frac{\exp\left[-\frac{E_s}{N_0}(1-\cos\frac{\pi}{M}\cos t)\right]}{1-\cos\frac{\pi}{M}\cos t}\,dt \\ P_{b,\,\mathrm{CD}} = \frac{a(M)}{\log_2 M}\,\mathrm{erfc}\left(\sqrt{\frac{E_s}{N_0}}\sin\frac{\pi}{M}\right) \cdot \left[1 - \frac{1}{2}\,\mathrm{erfc}\left(\sqrt{\frac{E_s}{N_0}}\sin\frac{\pi}{M}\right)\right] \end{cases} \quad (24)$$

which are approximation for $M \ge 8$.

C. Numerical Results

We calculated the BER performances of 2 and 4DPSK with DF-DPD using (23) and those with conventional DPD and CD using (24). The results are plotted in Figs. 5 and 6 as a function of E_b/N_0. The difference in the required E_b/N_0 values at BER $= 10^{-3}$ between conventional DPD and CD is 1.8 (0.6) dB for 4 DPSK (2DPSK). It is clearly seen that the performance improves as L increases and approaches that of CD. The performance improvement for $L = 4$ at BER $= 10^{-3}$ is 1.2 (0.5) dB for 4 DPSK (2DPSK). The performance with $L = 10$ equals that of CD to within 0.2 (0.04) dB for 4 DPSK (2DPSK).

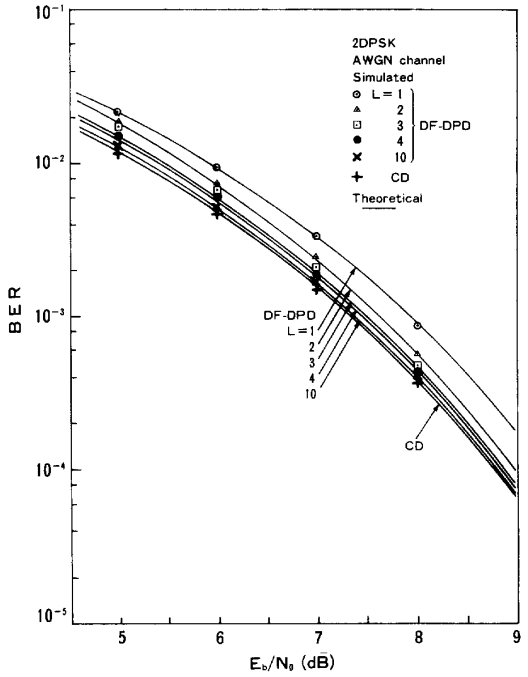

Fig. 5. BER of DF-DPD for 2DPSK.

IV. Computer Simulations

The BER performance of DF-DPD is evaluated by computer simulations for 2DPSK and 4DPSK transmission in AWGN and Rayleigh fading channels. DF-DPD performance is also compared with other multiple-symbol detection schemes: ML-DD, Viterbi-DD, and DF-DD.

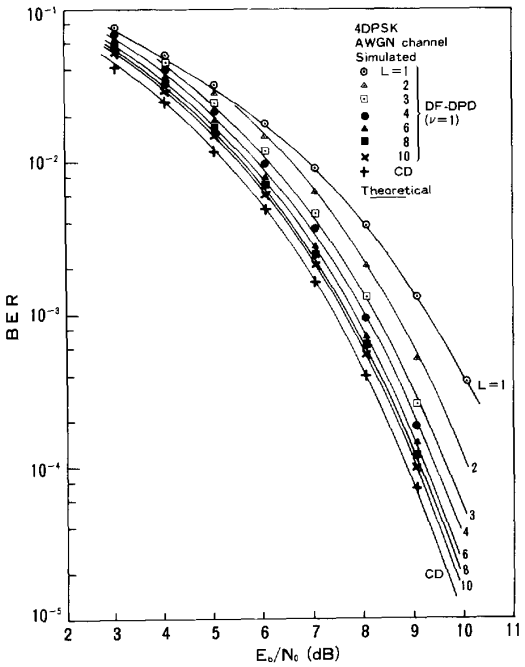

Fig. 6. BER of DF-DPD for 4DPSK.

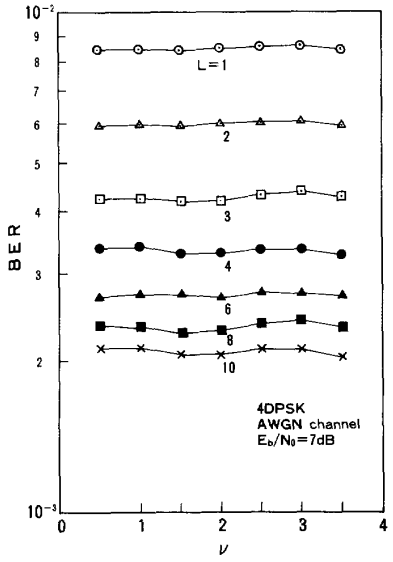

Fig. 7. Impact of ν on BER.

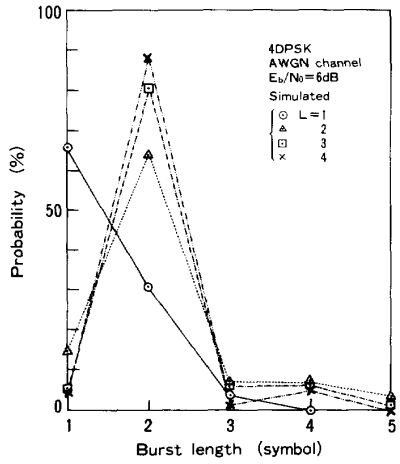

Fig. 8. Burst error probability.

A. AWGN Channel

We adopted the Gaussian phase noise assumption and derived the DF-DPD algorithm in Section II. However, the DPD detector output noise is not exactly Gaussian, so the raising factor of 2 of the phase errors may not be optimum. In general, we may be able to use the sum of the νth (> 0) power of the absolute values of phase errors. Accordingly, the decision rule of (13) is modified to

$$\Delta\bar{\phi}_n = \min_{\text{over}\,\Delta\phi_n} \sum_{l=1}^{L} |\mu_l|^{\nu}. \tag{25}$$

The impact of ν on BER was investigated for 4DPSK in the AWGN channel and the results are plotted in Fig. 7 for various values of L at $E_b/N_0 = 7$ dB. It can be seen that the BER performance is almost insensitive to the value of ν; the selection of ν is not important. By choosing $\nu = 1$, multiplication operations are not necessary and the algorithm can be performed using addition operations only. This reduces the computation complexity of DF-DPD significantly. Thus, in the following, we use $\nu = 1$.

In Section III, we showed that decision feedback most likely produces double-symbol errors. To confirm this, we measured the probability of n-symbol solid burst error with n being integer. The solid burst error is defined as consecutive symbol errors between correctly detected symbols (at least one symbol). The measured result at $E_b/N_0 = 6$ dB is shown in Fig. 8. Double-symbol errors occur with large probability (30.8%) even for conventional DPD; the reason is well explained in [10]. Double-symbol errors are much more predominant in the decision feedback scheme. The probability of double-symbol errors is 64.1% when $L = 2$. It increases with L, reaching 94.4% when $L = 10$.

The simulation results for the BER performance with DF-DPD are plotted in Figs. 5 and 6. It is seen that the simulation results are in good agreement with the theoretically predicted BER values; the approximate expression derived in Section III is very accurate. We also computer-simulated ML-DD [1], Viterbi-DD [2], and DF-DD [5], and compared their performance improvements with that of the proposed DF-DPD. It is shown [7] that the approximate BER performance of DF-DD[1] is equal to the BER upper bound of ML-DD. We can show that the expression for the BER of DF-DPD is also identical to that of DF-DD (compare (23) to [7, Eq. (3)]). This implies that DF-DPD, DF-DD, and ML-DD provide almost the same

[1]The exact BER expression of DF-DD with correct symbol feedback was derived by Edbauer [5]. Multiplying it by two gives an approximate BER when taking into account error propagation.

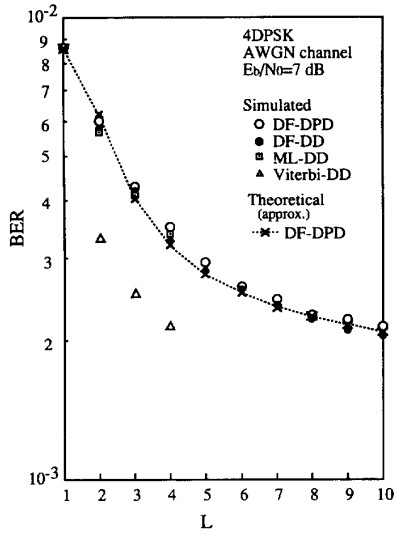

Fig. 9. Performance comparison.

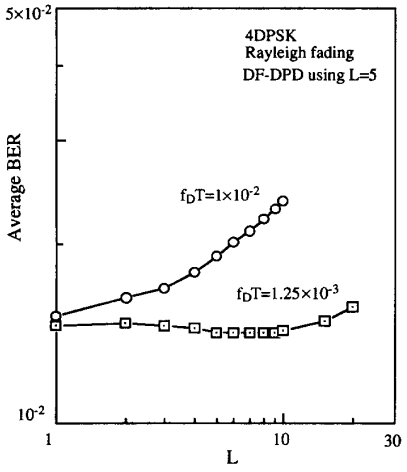

Fig. 10. Dependence of the average BER on L under Rayleigh fading.

BER performance. To confirm this, we plotted the simulated BER's, as well as theoretically predicted approximate BER's of DF-DPD calculated from (23), at $E_b/N_0 = 7$ dB in Fig. 9. Although DF-DPD provides slightly larger BER's than ML- and DF-DD, we found that the performance difference in the required E_b/N_0 for 10^{-3} less than 0.1 dB. Also plotted are the BER's achieved by Viterbi-DD (20-symbol decoding depth). It is seen from Fig. 9 that our DF-DPD using $L = 4$, 6, and 10 corresponds to Viterbi-DD using $L = 2$, 3, and 4, respectively.

B. Rayleigh Fading Channel

The BER performance of 4DPSK was evaluated. A frequency-nonselective (multiplicative) Rayleigh faded signal was generated based on Jakes model [11] assuming constant amplitude 16 multipaths. The BER dependence on L is plotted in Fig. 10 for $f_DT = 1.25 \times 10^{-3}$ and 1×10^{-2}, where f_D is the maximum Doppler frequency given by traveling

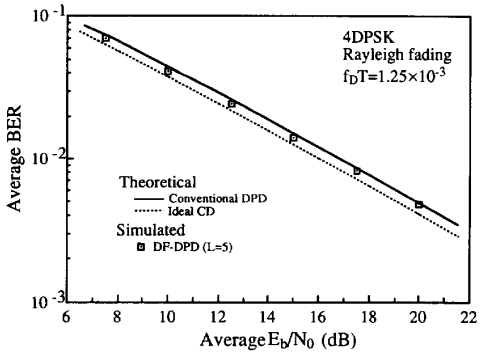

Fig. 11. Average BER performance under Rayleigh fading.

speed/carrier wavelength.[2] The simulated BER's of DF-DPD using $L = 5$ are plotted as a function of average E_b/N_0 in Fig. 11 for $f_DT = 1.25 \times 10^{-3}$. For comparison, the theoretical BER performances of conventional DPD and ideal CD (the perfect knowledge of random phase variations is assumed) are also shown as the solid line and dotted line, respectively. The BER performances of 4DPSK using conventional DPD and CD for very slow Rayleigh fading are obtained by averaging (24) with the exponentially distributed E_b/N_0 $(= 0.5(E_s/N_0))$ as

$$P_{b,\,\text{conventional DPD}} = \frac{1}{2}\left[1 - \frac{1}{\sqrt{2\left(1+\frac{1}{2\Gamma}\right)^2 - 1}}\right]$$

$$P_{b,\,\text{CD}} = \frac{1}{2}\left[1 - 2\frac{1 - \frac{2}{\pi}\tan^{-1}\sqrt{1+\frac{1}{\Gamma}}}{\sqrt{1+\frac{1}{\Gamma}}}\right] \tag{26}$$

where Γ is the average E_b/N_0. The decision feedback scheme assumes that the random phase θ of the received signal remains almost constant over the time duration of $(L+1)T$. In fading environments, however, θ fluctuates. Furthermore, most errors are produced in small E_b/N_0 regions, say, less than 3 dB, where the improvement obtained by the algorithm is small (see Figs. 5 and 6). For these reasons, DF-DPD only slightly (by a fraction of dB) improves the BER performance for the case of very slow fading $(f_DT = 1.25 \times 10^{-3})$. For the case of fast fading $(f_DT = 1 \times 10^{-2})$, the conventional DPD $(L = 1)$ provides better performance than DF-DPD.

V. Conclusion

We have presented a decision feedback multiple-symbol DPD (DF-DPD) scheme for M-ary DPSK. The idea of decision feedback [5], [6] was applied to differential phase detection (DPD). The results obtained in this paper are summarized as follows. 1) Adopting a Gaussian phase noise assumption, we derived the DF-DPD decision algorithm based on feeding back the $L - 1$ past detected symbols and minimizing the sum of the squared phase errors of 1 to L-symbol

[2] Assuming 1 GHz carrier frequency and 32 ksymbol/s transmission rate, the normalized Doppler spread of $f_DT = 1.25 \times 10^{-3}(1 \times 10^{-2})$ corresponds to a traveling speed of 43.2 (345.6) km/h.

DPD detectors. 2) An accurate approximate BER expression for DF-DPD in the AWGN channels was derived. It was shown that if the nine past detected symbols are fedback ($L = 10$), the BER performance in the AWGN channel approaches that of CD within 0.2 (0.04) dB for 4DPSK (2DPSK). 3) A practical implementation of the DF-DPD receiver that recursively generates the phase errors from the conventional DPD detector output was presented. It was shown that decision can be based on the sum of the *absolute* phase errors instead of the squared phase errors with no performance degradation; thus, only one-dimensional modulo-2π phase addition operations are required. 4) The application limitation of DF-DPD in Rayleigh fading environments was discussed. DF-DPD slightly improves the BER performance for the case of very slow fading; for the case of very fast fading, the conventional DPD ($L = 1$) provides better performance than DF-DPD.

APPENDIX

A phasor diagram showing the sum of the signal and noise vectors is shown in Fig. 2. The detected phase ψ_n fluctuates around $\phi_n + \theta$ due to AWGN. The exact pdf of the AWGN-induced phase noise η_n is shown in [8, Eqs. (67) and (68)]. We will show below that the pdf of η_n can be approximated as a Gaussian distribution for large E_s/N_0. Referring to Fig. 2, we introduce a new variable ξ_n defined as $\xi_n = w_n \exp -j(\phi_n + \theta)$; ξ_n becomes a zero-mean complex Gaussian variable with variance $2N_0/T$. Since

$$\eta_n = \tan^{-1}\left(\frac{\mathrm{Im}\,[\xi_n]}{\sqrt{\frac{2E_s}{T}} + \mathrm{Re}\,[\xi_n]}\right) \tag{A1}$$

the following approximation holds for large E_s/N_0:

$$\eta_n \approx \frac{\mathrm{Im}\,[\xi_n]}{\sqrt{\frac{2E_s}{T}}} \tag{A2}$$

where $\mathrm{Re}\,[z]$ and $\mathrm{Im}\,[z]$ are the real and imaginary parts of the complex value z, respectively. Since $\mathrm{Im}\,[\xi_n]$ is a zero-mean Gaussian variable with variance N_0/T, η_n becomes a Gaussian variable with variance $0.5(E_s/N_0)^{-1}$. Noting that w_n's are uncorrelated, η_n's can also be approximated as uncorrelated, zero-mean Gaussian variables with the same variance $0.5(E_s/N_0)^{-1}$.

REFERENCES

[1] D. Divsalar and M. K. Simon, "Multiple-symbol differential detection of MPSK," *IEEE Trans. Commun.*, vol. 38, pp. 300–308, Mar. 1990.

[2] D. Makrakis and K. Feher, "Optimal noncoherent detection of PSK signals," *Electron. Lett.*, vol. 26, pp. 398–400, Mar. 1990.

[3] D. Makrakis, A. Yongacoglu, and K. Feher, "Novel receiver structures for system using differential detection," *IEEE Trans. Vehic. Technol.*, vol. VT-36, pp. 71–77, May 1987.

[4] F. Adachi and M. Sawahashi, "Viterbi-decoding differential detection of DPSK," *Electron. Lett.*, vol. 28, pp. 2196–2197, Nov. 1992.

[5] F. Edbauer, "Bit error rate of binary and quaternary DPSK signals with multiple differential feedback detection," *IEEE Trans. Commun.*, vol. 40, pp. 457–460, March 1992.

[6] H. Leib and S. Pasupathy, "The phase of a vector perturbed by Gaussian noise and differentially coherent receivers," *IEEE Trans. Inform. Theory*, vol. 34, pp. 1491–1501, Nov. 1988.

[7] F. Adachi and M. Sawahashi, "Decision feedback multiple-symbol differential detection for M-ary DPSK," *Electron. Lett.*, vol. 29, pp. 1385–1387, July 1993.

[8] R. F. Pawula, S. O. Rice, and J. H. Roberts, "Distribution of the phase angle between two vectors perturbed by Gaussian noise," *IEEE Trans. Commun.*, vol. COM-30, pp. 1828–1841, Aug. 1982.

[9] P. J. Lee, "Computation of the bit error rate of coherent M-ary PSK with Gray code bit mapping," *IEEE Trans. Commun.*, vol. COM-34, pp. 488–491, May 1986.

[10] J. Goldman, "Multiple error performance of PSK systems with cochannel interference and noise," *IEEE Trans. Commun.*, vol. COM-19, pp. 420–430, Aug. 1971.

[11] W. C. Jakes, Jr., Ed., *Microwave Mobile Communications.* New York: Wiley, 1974.

Fumiyuki Adachi (M'79–SM'90) graduated from Tohoku University, Japan, in 1973 and received the Dr. Engineering degree from the same university in 1984.

In 1973, he joined the Nippon Telegraph & Telephone Corporation (NTT) Laboratories in Japan and in 1992, he transferred to NTT Mobile Communications Network, Inc. Since joining NTT, he has been doing research in the areas of CDMA/TDMA mobile radio communications systems and digital signal processing, including bandwidth efficient modulation/demodulation, diversity reception, and channel coding. During the academic year 1984–1985, he was United Kingdom SERC Visiting Research Fellow at the Department of Electrical Engineering and Electronics of Liverpool University. He has authored chapters in three books: Y. Okumura and M. Shinji, Eds., *Fundamentals of Mobile Communications* (in Japanese), (IEICE Japan, 1986), M. Shinji, Ed., *Mobile Communications* (in Japanese), (Maruzen, 1989), and M. Kuwabara, Ed., *Digital Mobile Communications* (in Japanese), (Kagaku Shinbun-sha, 1992).

Dr. Adachi has been a Secretary of the IEEE Vehicular Technology Society Tokyo Chapter since 1991. He is a co-recipient of the IEEE Vehicular Technology Society Paper of the Year Award in 1980 and 1990.

Mamoru Sawahashi (M'89) was born in Kanagawa, Japan, in 1959. He received the B.S. and M.S. degrees from Tokyo University, Tokyo, Japan, in 1983 and 1985, respectively.

In 1985 he joined NTT Laboratories, and in 1992 he transferred to NTT Mobile Communications Network, Inc. Since joining NTT, he has been engaged in the research of mobile radio communication systems. He is now a Senior Research Engineer with the Research and Development Department of NTT Mobile Communications Network, Inc.

Mr. Sawahashi is a member of the Institute of Electronics, Information, and Communication Engineers of Japan.